

# Facile Fabrication of Efficient Organic CMOS Circuits

Andrzej Dzwilewski,<sup>†</sup> Piotr Matyba, and Ludvig Edman\*

The Organic Photonics and Electronics Group, Department of Physics, Umeå University, SE-901 87 Umeå, Sweden

Received: September 24, 2009

Organic electronic circuits based on a combination of n- and p-type transistors (so-called CMOS circuits) are attractive, since they promise the realization of a manifold of versatile and low-cost electronic devices. Here, we report a novel photoinduced transformation method, which allows for a particularly straightforward fabrication of highly functional organic CMOS circuits. A solution-deposited single-layer film, comprising a mixture of the n-type semiconductor [6,6]-phenyl-C<sub>61</sub>-butyric acid methyl ester (PCBM) and the p-type semiconductor poly-3-hexylthiophene (P3HT) in a 3:1 mass ratio, was utilized as the common active material in an array of transistors. Selected film areas were exposed to laser light, with the result that the irradiated PCBM monomers were photochemically transformed into a low-solubility and high-mobility dimeric state. Thereafter, the entire film was developed via immersion into a developer solution, which selectively removed the nonexposed, and monomeric, PCBM component. The end result was that the transistors in the exposed film areas are n-type, as dimeric PCBM is the majority component in the active material, while the transistors in the nonexposed film areas are p-type, as P3HT is the sole remaining material. We demonstrate the merit of the method by utilizing the resulting combination of n-type and p-type transistors for the realization of CMOS inverters with a high gain of ~35.

## I. Introduction

The current generation of electronic devices is primarily based on inorganic semiconductors such as silicon, but during the last years, organic semiconductors (OSCs) have emerged as a promising alternative for applications where low cost, flexibility, large-area coverage, and/or novel function are considered beneficial.<sup>1–16</sup> The field-effect transistor (FET) is a particularly important electronic device, as it is exploited in a manifold of ubiquitous applications, ranging from the switching element in flat-panel displays to the amplifier in speakers and microphones. FETs are commonly divided into two different classes: n-type when the charge transport in the active material is carried out by electrons and p-type when the charge transport is carried out by holes. A combination of n-type and p-type FETs with similar charge-transport mobility is the basis for the complementary-metal-oxide-semiconductor (CMOS) technology. CMOS circuits exhibit a number of important advantages, including good fault tolerance, high noise immunity, and low power consumption, and they are accordingly utilized in a broad range of analog and digital logic applications.

Currently, there is a strong interest in the realization of organic CMOS circuits, which combine the attractive characteristic features of OSCs with the efficient operation that the CMOS technology offers.<sup>7,17–25</sup> However, a significant hurdle in this pursuit stems from the fact that while inorganic FETs can conveniently be manipulated into either p-type or n-type operation via chemical doping of selected regions of the active material, this is not commonly a practical option in OSCs, due to the significant diffusivity of the dopant counterions in a soft organic material.<sup>26,27</sup> Thus, in order to realize functional organic

CMOS circuits, it is necessary to develop new fabrication schemes, which consider and exploit the specific properties of OSCs; some recent examples include gate–dielectric interface engineering,<sup>27–29</sup> employment of ambipolar active materials,<sup>18,30–36</sup> and spatially separated deposition of two different OSCs with complementary charge-transport capacity.<sup>17,23,37,38</sup>

In this Article, we demonstrate an alternative and potentially generic method for the fabrication of functional organic CMOS circuits, which is notably straightforward and scalable. We utilize a solution-processable designed blend between an n-type OSC and a p-type OSC as the common active material in an array of FETs. The n-type OSC can be photochemically converted into a low-solubility state with retained high mobility. By exposing selected FETs to laser light, and then developing the entire array with a tuned developer solution, we are able to attain a combination of (exposed) n-type FETs and (nonexposed) p-type FETs with balanced charge-transport mobility. The merit of the technique is manifested in the fabrication of fully functional CMOS-like inverter stages with a high gain of 35.

## II. Experimental Methods

The FET devices were fabricated in a bottom-gate configuration using a highly p-type doped Si wafer as a combined substrate and gate electrode, and utilizing a 200 nm thin layer of thermally grown SiO<sub>2</sub> as the gate dielectric ( $C = 1.73 \times 10^{-4}$  F/m<sup>2</sup>). The gate dielectric was exposed to a saturated vapor of hexamethyldisilazane (HMDS) for 3 h, prior to the deposition of the active material.

[6,6]-Phenyl-C<sub>61</sub>-butyric acid methyl ester (PCBM, >99.5%, Solenne) and regioregular poly-3-hexylthiophene (P3HT, 99.995%,  $M_n \sim 17500$  g/mol, Sigma-Aldrich) were separately dissolved in anhydrous chlorobenzene (99.8%, Sigma-Aldrich) in a concentration of 20 mg/mL. The master solutions were stirred for 5 h at  $T = 323$  K, and thereafter mixed together in various PCBM:P3HT volumetric ratios. The mixed solutions

\* Corresponding author. Phone: +46-9-7865732. Fax: +46-90-7866673. E-mail: ludvig.edman@physics.umu.se.

<sup>†</sup> Current address: Molecular Materials and Nanosystems, Eindhoven University of Technology, P.O. Box 513, 5600 MB Eindhoven, The Netherlands.

were stirred for 5 h at  $T = 323$  K, before being spin-coated (acceleration, 100 rpm/s; speed, 800 rpm; time, 60 s) onto the HMDS-treated gate dielectric on top of the transistor substrates. The spin-coated active material films were annealed for 1–3 min at  $T = 375$  K, as we found that this specific treatment resulted in the best transistor performance. Au electrodes were thermally evaporated on top of the active material under high vacuum ( $p < 5 \times 10^{-6}$  mbar). A shadow mask was utilized to define a channel length of  $L = 110 \mu\text{m}$  and a channel width of  $W = 1.2$  mm.

After fabrication, the FET devices were kept under a  $\text{N}_2$  atmosphere for at least 5 h before characterization and/or further treatment was carried out, as we find that the device performance varies slightly during the first 5 h of storage, where after it remains stable. The laser-light exposure of selected regions of the active material film was executed for a time period of 1 h, using a green-emitting solid-state laser ( $\lambda = 532$  nm,  $\sim 16$  mW/mm<sup>2</sup>). (Other laser wavelengths that are strongly absorbed by PCBM can also be utilized for the photochemical conversion process.<sup>39</sup>) The development was performed by immersing the entire substrate for  $\sim 30$  s into a carefully tuned developer solution comprising chloroform and acetone in a 1:7 volumetric ratio. After the development, the devices were dried for 15 min at  $T = 323$  K. The characterization of FET devices was carried out using a Keithley 4200 Semiconductor Characterization System, with the source electrode grounded. All fabrication steps and measurements were performed under a  $\text{N}_2$  atmosphere ( $\text{O}_2$ ,  $\text{H}_2\text{O} < 1$  PPM) in two interconnected glove boxes with an integrated thermal evaporator.

The samples for the absorption spectroscopy measurements were fabricated and prepared in an identical manner as the active material films in the FET devices, as detailed above. The samples were then transferred to an optical-access vacuum chamber, equipped with two fused silica window ports (thickness = 3 mm), in which a high vacuum ( $p < 1 \times 10^{-4}$  mbar) was established before the measurements were carried out. For the recording of optical absorption spectra, a high speed spectrometer (HR4000, entrance aperture =  $5 \mu\text{m}$ , grating range = 200–1100 nm, Ocean Optics) and a tungsten halogen lamp (HL-2000-HP-232, Ocean Optics), both computer controlled with the Spectral Suite software via the RS232 port, were utilized. The absorption spectra were recorded with an integration time of 190 ms, and background effects (stemming, e.g., from the influence of the substrate and stray light) were corrected for via the parallel acquisition of background spectra. The herein presented absorption spectra are averages of 10 such independent measurements.

### III. Results and Discussion

We have recently demonstrated a photoinduced and resist-free patterning technique,<sup>39</sup> which exploits an attractive combination of properties of fullerene materials: (i) they can form oligomeric and polymeric structures during exposure to laser light,<sup>40–43</sup> (ii) the exposed and chemically modified material exhibits a distinctly lowered solubility in tuned developer solutions as compared to the pristine material,<sup>44,45</sup> and (iii) the laser-exposed (and subsequently solution-developed) material exhibits an essentially intact electron mobility.<sup>39,46</sup> Thus, by exposing selected regions of a fullerene film to laser light, and then developing the entire film in a developer solution, a pattern of electronically active fullerene material defined by the incident laser beam is created. The merit of the technique has been demonstrated by the facile patterning of *single-component* PCBM and  $\text{C}_{60}$  films into well-defined arrays of fully functional n-type FETs.<sup>39,46</sup>

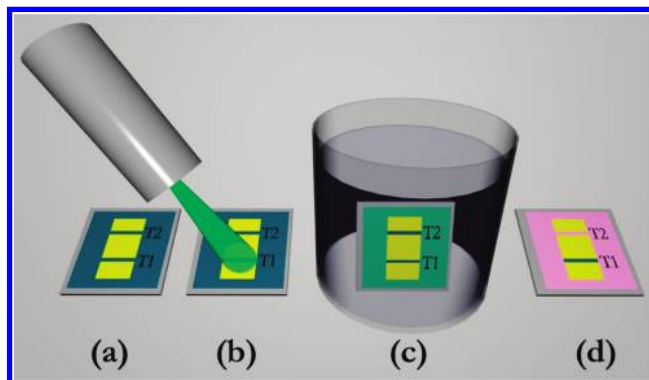


**Figure 1.** Schematic presenting the key steps in the photoinduced transformation technique. (a)  $2 \times 1$  array of field-effect transistors with a pristine active material film comprising a binary blend of a fullerene compound and a complementary organic semiconductor (c-OSC). The two transistors are termed T1 and T2. (b) Transistor T1 is irradiated by laser light during the exposure step. (c) The entire substrate with both transistors is immersed into a solution during the development step. (d) The end result is that both components in the active material remain in the channel of the exposed and developed transistor T1, while solely the c-OSC remains in the channel of the developed transistor T2 (and the rest of the nonexposed regions of the blend film).

Here, we demonstrate that the attractive combination of properties of fullerene materials also can be exploited for the tuning of composition and property (e.g., n-type or p-type) features in selected areas of a semiconductor *blend* film. Figure 1 illustrates the key constituent steps of the method as applied on a (dark blue) blend film, which acts as the common active material in a  $2 \times 1$  array of transistors termed T1 and T2. The film comprises a combination of a fullerene compound that changes its solubility after laser exposure, and a “complementary” organic semiconductor (c-OSC) that is effectively unaffected by both the laser exposure and the solvent development. In Figure 1b, the active material in T1 is exposed to the laser light, which causes the fullerene compound to change its solubility while the c-OSC is left unaffected. In Figure 1c, the entire film is dipped into a developer solution, which selectively removes the nonexposed fullerene compound. The end result of the exposure-development process is presented in Figure 1d, where the (dark blue) blend of the fullerene and c-OSC remains in the exposed area (i.e., the active material of T1), and solely the (light pink) c-OSC remains in the nonexposed regions (including the active material of T2). Accordingly, if the pristine blend is designed (e.g., via the composition) so that the properties of the fullerene compound dominate, then transistor T1 will exhibit properties reflecting the exposed fullerene compound, while the properties of transistor T2 are single-handedly determined by the c-OSC.

Here, we have utilized n-type PCBM for the fullerene compound and p-type P3HT for the c-OSC, but other combinations of photochemically modifiable fullerene compounds and c-OSC are expected to function as well. A large number of transistors comprising active materials with varying PCBM: P3HT mass ratio have been investigated and characterized. We find that a PCBM:P3HT mass ratio of 3:1 fulfills the above outlined requirements in a satisfying manner, as such exposed and developed transistors are primarily n-type while solely developed transistors are p-type. Moreover, the recorded n-type and p-type mobilities are, as desired from a CMOS perspective, relatively well-balanced.

Transistor data for a typical device with a pristine (3:1) blend as the active material is presented in Figure 2. A qualitative analysis of the data reveals that the transistor indeed is primarily

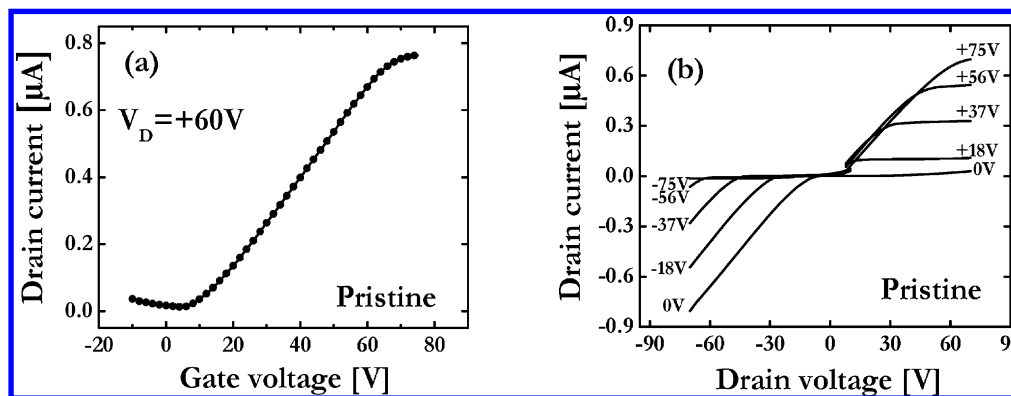


**Figure 2.** (a) Transfer characteristics and (b) output characteristics for a field-effect transistor with a pristine blend of PCBM:P3HT (mass ratio 3:1) as the active material. The gate voltages applied during the recording of the output data are indicated in part b.

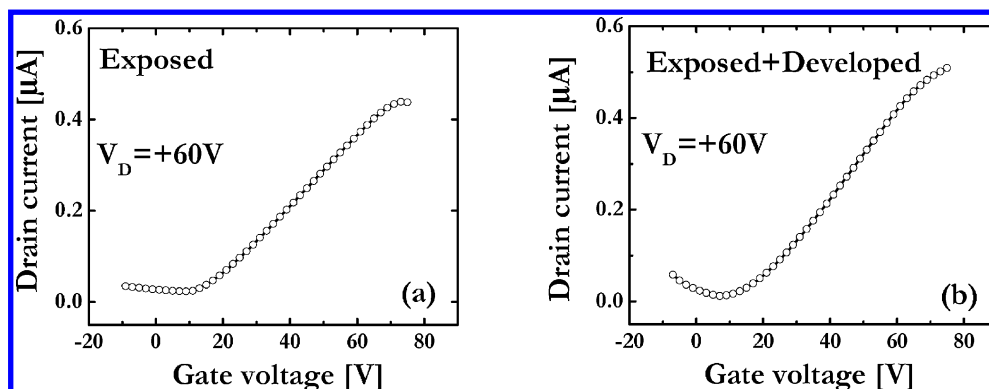


**Figure 3.** Transfer characteristics for transistor T1 in Figure 2 following (a) laser-light exposure of the active material and (b) the subsequent solution development.

n-type, as manifested in the fact that the transfer characteristics in Figure 2a exhibit a monotonously increasing drain current ( $I_D$ ) with increasing gate voltage ( $V_G$ ) when  $V_G > 0$  (at a drain voltage,  $V_D$ , of 60 V) and that the output characteristics in Figure 2b exhibit a clear saturation for  $I_D$  in the first quadrant when  $V_D > V_G$ . It is harder to find signs of p-type behavior, but a weak increase in  $I_D$  when  $V_G < 0$  in Figure 2a and a tendency to superlinear increase in  $I_D$  at large positive  $V_D$  when  $V_G = 0$  V in Figure 2b are consistent with a minor p-type behavior. The n-type behavior can be quantified by estimating the electron mobility ( $\mu_n$ ) in the saturation regime with the following equation:

$$I^{0.5} = \left( \frac{W \cdot C \cdot \mu}{2L} \right)^{0.5} \cdot (V_G - V_{TH}) \quad (1)$$

where  $W$  and  $L$  represent the transistor channel width and length, respectively,  $C$  is the capacitance per unit area of the gate dielectric, and  $V_{TH}$  is the threshold voltage. For a typical transistor with a pristine PCBM:P3HT blend film in a 3:1 mass ratio as the active material (e.g., the device in Figure 2), we calculate  $\mu_n = 3 \times 10^{-3} \text{ cm}^2/(\text{V s})$ .

The active material of the transistor in Figure 2 was thereafter first exposed to green laser light and then developed by immersion into a carefully tuned developer solution comprising a mixture of chloroform and acetone in a (1:7) volumetric ratio. In agreement with the terminology of Figure 1, we chose to term this transistor T1. The transfer characteristics of T1 after the exposure, and after the subsequent development, are presented in parts a and b of Figure 3, respectively. We find that the electronic properties of a typical (3:1) blend film are left essentially intact following each step in the exposure-development treatment, as the hole mobility is still negligible

and the electron mobility remains relatively high;  $\mu_n$  (pristine film) =  $3 \times 10^{-3} \text{ cm}^2/(\text{V s})$  vs  $\mu_n$  (exposed and developed film) =  $2 \times 10^{-3} \text{ cm}^2/(\text{V s})$ .

A second transistor on the same substrate, termed T2 in analogy with Figure 1, was immersed into the developer solution without any preceding laser exposure of the active material. Figure 4a shows the transfer characteristics of T2 before the development (i.e., with a pristine active material), and the device is, as previously observed, primarily n-type. (A comparison between Figure 2a and the inset in Figure 4a visualizes an example of the good repeatability of the measurements.) Parts b and c of Figure 4 present the transfer characteristics and the output characteristics, respectively, after the development. A striking change in behavior following the development is observed, as the initially primarily n-type device has transformed into a solely p-type device. The transfer data in Figure 4b exhibit a monotonous increase for  $I_D$  with decreasing  $V_G$ , and the output data in Figure 4c exhibit clear saturation in the third quadrant and a superlinear behavior in the first quadrant, all of which are characteristic signatures of a p-type device. By utilizing eq 1, we find that  $\mu_p = 1.4 \times 10^{-3} \text{ cm}^2/(\text{V s})$  is a typical hole mobility for such a device after the development.

If we now summarize the measured transistor data, we find that they are consistent with the desired scenario, as outlined in Figure 1. The exposure of the active material in T1 transforms the PCBM component from a high-solubility state to a low-solubility state (Figure 1b). The subsequent development dissolves the nonexposed, high-solubility PCBM in the active material of T2 (and the surrounding regions) while leaving the P3HT and the exposed, low-solubility PCBM in T1 intact (Figure 1c). The end result following the exposure-development



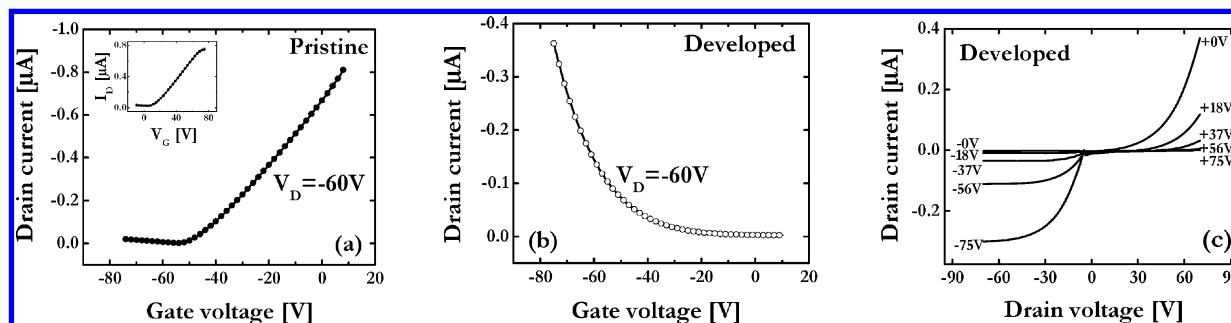


**Figure 4.** (a) Transfer characteristics for transistor T2 with a pristine blend of PCBM:P3HT (mass ratio 3:1) as the active material. The transfer characteristics in the inset were recorded at  $V_D = +60$  V. (b) Transfer characteristics and (c) output characteristics for the same transistor T2 after the active material had been developed without any preceding exposure to laser light. The gate voltages applied during the recording of the output data are indicated in part c.

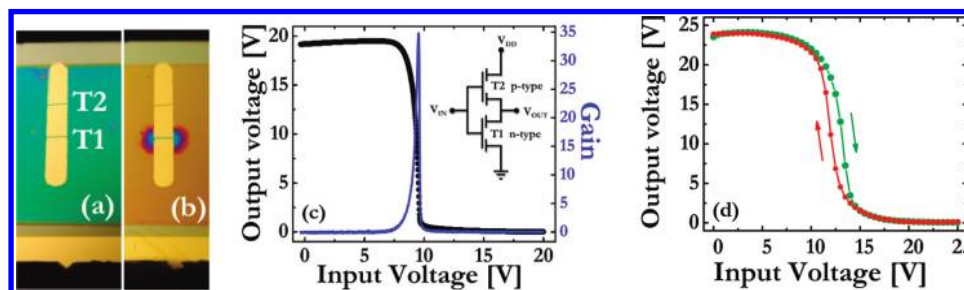


**Figure 5.** (a) Photograph of a substrate comprising two transistors T1 and T2, which utilize the same (green) pristine PCBM:P3HT (3:1) film as the active material. (b) Photograph of the same substrate after the selective laser-light exposure of the film region including and surrounding the channel of transistor T1, and the subsequent solution development of the entire substrate. (c) The transfer characteristics (left, solid circles) and the gain (right, blue line) of a CMOS inverter fabricated from the transistors T1 and T2 in part b in accordance with the schematic in the inset. (d) The transfer characteristics of an inverter during back-and-forth scanning at a scan rate of  $|dV_{IN}/dt| = 1$  V/s. Note that  $V_{DD} = 20$  V in part c and  $V_{DD} = 25$  V in part d.

cycle is thus that transistor T1 comprises a combination of PCBM and P3HT, where the former dominates, while transistor T2 comprises solely P3HT. This scenario is manifested in the fact that transistor T1 remains n-type (see Figure 3) and that transistor T2 has transformed into being p-type (see Figure 4b and c). It is further notable that both the p-type transistors and the n-type transistors demonstrate good injection properties, as indicated by the linear dependence of the drain current on drain voltage at low drain voltages (see first quadrant in Figure 2b and third quadrant in Figure 4c),<sup>47</sup> despite the fact that Au was used for both the source and the drain electrodes.

Directly visible evidence that our proposed scenario is correct should be provided by optical imaging, as a selective removal of the majority PCBM component from the nonexposed regions should result in a clearly distinguishable optical contrast between the (thick) exposed and developed regions and the (thin) solely developed regions. Figure 5a presents a photograph of a pristine blend film, which functions as the common active material in two transistors T1 and T2. Figure 5b presents a photograph of the same film after the material including and surrounding the channel of transistor T1 had been exclusively exposed to laser light and the entire film thereafter had been developed. It is clear that the visual appearance of the pristine film and the exposed and developed film are very similar, while the appearance of the solely developed active material is distinctly different. This serves as further confirmation that the exposure step transforms the PCBM material from a high-solubility state to a low-solubility state, and that the nonexposed PCBM component is selectively removed by the developer solution.

We now shift our attention to the opportunity that unipolar n-type and p-type transistors with balanced charge-transport properties (i.e., similar mobility) offer in the context of CMOS circuits. We have connected the n-type transistor T1 and the

p-type transistor T2 in Figure 5b in accordance with the circuit diagram of a CMOS inverter stage, as presented in the inset of Figure 5c. The supply voltage was set to  $V_{DD} = 20$  V. The output voltage ( $V_{OUT}$ ) response of the inverter during an input voltage ( $V_{IN}$ ) scan ranging from 0 to 20 V is presented in Figure 5c. As desired from a functional logic inverter, at low input voltage ( $V_{IN} < 8$  V), the inverter responds with an essentially constant high  $V_{OUT}$  approximately equal to the supply voltage, and at high input voltage ( $V_{IN} > 10$  V), the inverter responds with a constant low output signal of  $V_{OUT} = 0$  V. Moreover, the transition from high to low output voltage is rather sharp, as quantified by a high maximum gain (defined as the maximum absolute value of the derivative of the output voltage with respect to the input voltage) value of 35. A search in the literature reveals that this maximum gain value compares well with published results on organic inverter stages fabricated with alternative techniques.<sup>18,19,27–29,31–33,36–38</sup> We have also investigated the transient response of the inverter stage, as presented in Figure 5d, and it exhibits negligible hysteresis effects at a scan speed of  $|dV_{IN}/dt| = 1$  V/s. It should be noted that a faster temporal response can be expected via an improved device design, notably via a decreased physical overlap of the source-drain electrodes and the gate electrode and a concomitant decrease in the parasitic capacitance of the device.

We have fabricated and tested  $\sim 40$  inverter circuits in total, and the repeatability of the experiments must be considered to be very good, as  $\sim 90\%$  of the devices demonstrate appropriate inverter functionality and high gain. Those inverters that did not function satisfactorily were typically “over-developed”, in the sense that a significant fraction of the exposed PCBM material (in transistor-type T1) was removed during the (too long) development step. This had the undesired consequence that the exposed and developed transistor T1 exhibited a

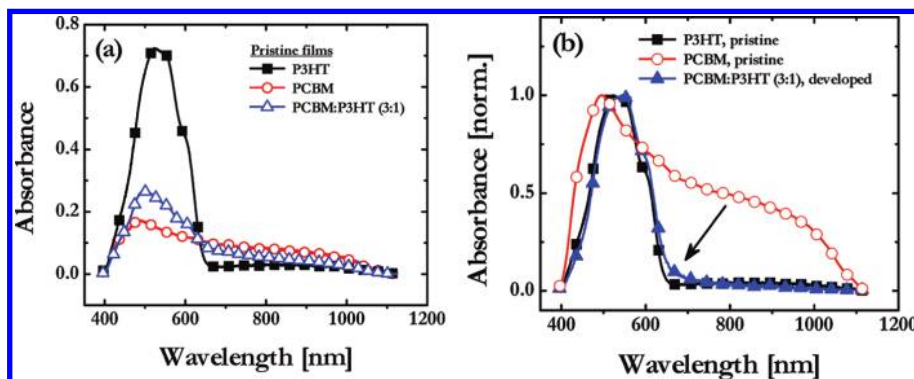


**Figure 6.** (a) Absorption spectra of a pristine P3HT film, a pristine PCBM film, and a pristine PCBM:P3HT (3:1) film. (b) Normalized absorption spectra for pristine P3HT and PCBM films, and a solely developed PCBM:P3HT (3:1) blend film. The arrow indicates the distinct low-energy shoulder that distinguishes the developed blend film from the pristine P3HT film.

significant bipolar character, and that  $V_{OUT}$  therefore did not reach  $V_{DD}$  at low  $V_{IN}$  values during inverter operation. The storage stability of the inverters under a  $N_2$  atmosphere is good, as we find no detectable deterioration in device performance following more than 2 months of storage.

From a fabrication perspective, it is particularly notable and attractive that the active material was deposited from solution in one step, and that the same stable electrode material (here, Au) could be utilized for both the n-type and p-type transistors, without any indication of contact problems in the transistor data. Moreover, as the constituent fabrication steps—the deposition of the active material from solution, the exposure to laser light, and the solution development—all are both scalable and compatible with roll-to-roll production, it is plausible to envision that the herein demonstrated photoinduced transformation technique could allow for a high-speed production of complex and easily adjusted organic CMOS circuits on flexible substrates.

We finally focus our attention on an attempt at unraveling the more detailed mechanisms that are in effect during the photoinduced tuning of the active material blend. In an earlier publication, we demonstrated that laser exposure of a single-component PCBM film can result in the following: (i) the PCBM transforms from a monomeric to a dimeric state via a so-called  $[2 + 2]$  cyclo-addition mechanism; (ii) the dimeric compound exhibits a distinctly lowered solubility as compared to the monomeric compound; (iii) the n-type mobility is essentially the same for both compounds.<sup>39</sup> Thus, considering the herein presented transistor data, we find it reasonable to propose that the laser exposure of a blend film between PCBM and P3HT, where the former is the majority component in a 3:1 mass ratio, transforms the PCBM into a dimeric state with low solubility. Accordingly, in the exposed and developed film, both the dimeric PCBM and the P3HT remains, while in the solely developed film only P3HT remains, as the monomeric PCBM is removed by the developer solution. It is interesting to note that the high p-type mobility in the solely developed film as compared to the pristine film (compare Figure 4b and c with Figure 2) indicates that the remaining (p-type) P3HT material has reorganized during the development step, when the PCBM majority component is removed, and adopted an improved morphology in the context of facile hole transport.

Further support for the above outlined scenario, and insight into the mechanism behind the improved p-type mobility in the P3HT phase following development, is provided by absorption spectroscopy. Figure 6a presents absorption spectra recorded on a pristine P3HT film (black solid squares), a pristine PCBM film (red open circles), and a pristine PCBM:P3HT blend film in a 3:1 mass ratio (blue open triangles). The P3HT film exhibits

the highest absorption in the visible range, with the peak absorption located at  $\sim 525$  nm, while the PCBM film demonstrates a broad absorption spectrum extending into the IR range. The pristine blend film exhibits an absorption spectrum, which as expected reflects the existence of both constituents and with the PCBM majority component as the dominant absorbing species.

Figure 6b presents the normalized absorption spectra for a pristine P3HT film, a pristine PCBM film, and a solely developed PCBM:P3HT blend film (blue filled triangles). We call attention to two important observations in the developed blend spectrum. First, the complete absence of absorption in the IR range (which is a distinguishing feature of PCBM in comparison to P3HT) in combination with the notable similarity to the pristine P3HT spectrum strongly indicates that the PCBM component is completely removed from the developed blend film. Second, a small but clearly distinguishable shoulder is observed at long wavelengths at  $\sim 600$ – $700$  nm in the developed blend film (indicated by the arrow) but not in the pristine P3HT film. It has been reported in the literature that the emergence of such a low-energy band at  $\sim 610$  nm in P3HT films correlates to an increase in the crystallinity.<sup>48–50</sup> Thus, we find it plausible to attribute the emergence of the distinct low-energy shoulder in the solely developed blend film to an increase in the crystallinity in the P3HT phase. This suggestion is also supported by the fact that the hole mobility in developed blend films is significantly higher than in their pristine counterparts, and the fact that the removal of the PCBM constituent opens up a large amount of free volume in the developed film, into which a “solvent-lubricated” P3HT polymer can relax and organize.

#### IV. Conclusions

To summarize, we exploit the fact that certain organic semiconductors can be photochemically transformed into a low-solubility state with retained high mobility for the realization of a novel and straightforward fabrication technique of efficient organic CMOS circuits. Specifically, we build an array of transistors with a solution-processed single-layer blend of the n-type fullerene PCBM and the p-type conjugated polymer P3HT (in a 3:1 mass ratio) as the common active material, and expose selected transistors to laser light. Following a subsequent development with a tuned developer solution, we attain a combination of (exposed) n-type transistors and (nonexposed) p-type transistors. With these complementary transistors it is possible to fabricate CMOS circuits, and we demonstrate the merit of the photoinduced transformation technique by realizing highly functional inverter stages with a high gain of 35.

**Acknowledgment.** The authors acknowledge Vetenskapsrådet and Umeå University for financial support. A.D. thanks Helge Ax:son Johnsons stiftelse for support. L.E. is a “Royal Swedish Academy of Sciences Research Fellow” supported by a grant from the Knut and Alice Wallenberg Foundation.

## References and Notes

- (1) Voss, D. *Nature* **2000**, *407*, 442–444.
- (2) Garnier, F.; Hajlaoui, R.; Yassar, A.; Srivastava, P. *Science* **1994**, *265*, 1684–1686.
- (3) Gelinck, G. H.; Huitema, H. E. A.; Van Veenendaal, E.; Cantatore, E.; Schrijnemakers, L.; Van der Putten, J.; Geuns, T. C. T.; Beenhakkers, M.; Giesbers, J. B.; Huisman, B. H.; Meijer, E. J.; Benito, E. M.; Touwslager, F. J.; Marsman, A. W.; Van Rens, B. J. E.; De Leeuw, D. M. *Nat. Mater.* **2004**, *3*, 106–110.
- (4) Sandberg, H. G. O.; Backlund, T. G.; Osterbacka, R.; Jussila, S.; Makela, T.; Stubb, H. *International Conference on Science and Technology of Synthetic Metals*; Elsevier Science Sa: Wollongong, Australia, 2004; pp 662–665.
- (5) Said, E.; Larsson, O.; Berggren, M.; Crispin, X. *Adv. Funct. Mater.* **2008**, *18*, 3529–3536.
- (6) Smits, E. C. P.; Mathijssen, S. G. J.; van Hal, P. A.; Setayesh, S.; Geuns, T. C. T.; Mutsaers, K.; Cantatore, E.; Wondergem, H. J.; Werzer, O.; Resel, R.; Kemerink, M.; Kirchmeyer, S.; Muzafarov, A. M.; Ponomarenko, S. A.; de Boer, B.; Blom, P. W. M.; de Leeuw, D. M. *Nature* **2008**, *455*, 956–959.
- (7) Zhang, X. H.; Potscavage, W. J.; Choi, S.; Kippelen, B. *Appl. Phys. Lett.* **2009**, *94*, 3.
- (8) Takamatsu, S.; Nikolou, M.; Bernards, D. A.; DeFranco, J.; Malliaras, G. G.; Matsumoto, K.; Shimoyama, I. *Sens. Actuators, B* **2008**, *135*, 122–127.
- (9) Logothetidis, S. *4th International Workshop on Nanoscience and Nanotechnologies*; Elsevier Science Bv: Thessaloniki, Greece, 2007; pp 96–104.
- (10) Na, S. I.; Kim, S. S.; Jo, J.; Kim, D. Y. *Adv. Mater.* **2008**, *20*, 4061–4067.
- (11) Winther-Jensen, B.; Krebs, F. C. *Sol. Energy Mater. Sol. Cells* **2006**, *90*, 123–132.
- (12) Shin, J. H.; Edman, L. *J. Am. Chem. Soc.* **2006**, *128*, 15568–15569.
- (13) Liu, B.; Bazan, G. C. *Nat. Protoc.* **2006**, *1*, 1698–1702.
- (14) Hamedi, M.; Herlogsson, L.; Crispin, X.; Marcilla, R.; Berggren, M.; Inganas, O. *Adv. Mater.* **2009**, *21*, 573+.
- (15) Berggren, M.; Nilsson, D.; Robinson, N. D. *Nat. Mater.* **2007**, *6*, 3–5.
- (16) Schmidt-Mende, L.; Fechtenkötter, A.; Mullen, K.; Moons, E.; Friend, R. H.; MacKenzie, J. D. *Science* **2001**, *293*, 1119–1122.
- (17) Crone, B.; Dodabalapur, A.; Lin, Y. Y.; Filas, R. W.; Bao, Z.; LaDuca, A.; Sarpeshkar, R.; Katz, H. E.; Li, W. *Nature* **2000**, *403*, 521–523.
- (18) Meijer, E. J.; De Leeuw, D. M.; Setayesh, S.; Van Veenendaal, E.; Huisman, B. H.; Blom, P. W. M.; Hummelen, J. C.; Scherf, U.; Klapwijk, T. M. *Nat. Mater.* **2003**, *2*, 678–682.
- (19) Wang, J.; Wei, B.; Zhang, J. H. *Semicond. Sci. Technol.* **2008**, *23*, 4.
- (20) Tatemichi, S.; Ichikawa, M.; Kato, S.; Koyama, T.; Taniguchi, Y. *Phys. Status Solidi RRL* **2008**, *2*, 47–49.
- (21) Kitamura, M.; Arakawa, Y. *Appl. Phys. Lett.* **2007**, *91*, 3.
- (22) Hizu, K.; Sekitani, T.; Someya, T.; Otsuki, J. *Appl. Phys. Lett.* **2007**, *90*, 3.
- (23) Ling, M. M.; Bao, Z. N.; Erk, P.; Koenemann, M.; Gomez, M. *Appl. Phys. Lett.* **2007**, *90*, 3.
- (24) Huang, C.; Katz, H. E.; West, J. E. *J. Appl. Phys.* **2006**, *100*, 9.
- (25) Opitz, A.; Bronner, M.; Brutting, W. *J. Appl. Phys.* **2007**, *101*, 9.
- (26) Shin, J. H.; Xiao, S.; Fransson, A.; Edman, L. *Appl. Phys. Lett.* **2005**, *87*, 043506.
- (27) Benson, N.; Melzer, C.; Schmechel, R.; von Seggern, H. *Phys. Status Solidi A* **2008**, *205*, 475–487.
- (28) Benson, N.; Schidleja, M.; Melzer, C.; Schmechel, R.; von Seggern, H. *Appl. Phys. Lett.* **2006**, *89*, 3.
- (29) Ahles, M.; Schmechel, R.; von Seggern, H. *Appl. Phys. Lett.* **2005**, *87*, 3.
- (30) Anthopoulos, T. D.; de Leeuw, D. M.; Cantatore, E.; Setayesh, S.; Meijer, E. J.; Tanase, C.; Hummelen, J. C.; Blom, P. W. M. *Appl. Phys. Lett.* **2004**, *85*, 4205–4207.
- (31) Hou, J. H.; Zhang, S. Q.; Chen, T. L.; Yang, Y. *Chem. Commun.* **2008**, 6034–6036.
- (32) Bronner, M.; Opitz, A.; Brutting, W. *Phys. Status Solidi A* **2008**, *205*, 549–563.
- (33) Chikamatsu, M.; Mikami, T.; Chisaka, J.; Yoshida, Y.; Azumi, R.; Yase, K.; Shimizu, A.; Kubo, T.; Morita, Y.; Nakasuji, K. *Appl. Phys. Lett.* **2007**, *91*, 3.
- (34) Takashima, W.; Murasaki, T.; Nagamatsu, S.; Morita, T.; Kaneto, K. *Appl. Phys. Lett.* **2007**, *91*, 3.
- (35) Wang, S. D.; Kanai, K.; Ouchi, Y.; Seki, K. *Org. Electron.* **2006**, *7*, 457–464.
- (36) Singh, T. B.; Senkarabacak, P.; Sariciftci, N. S.; Tanda, A.; Lackner, C.; Hagelauer, R.; Horowitz, G. *Appl. Phys. Lett.* **2006**, *89*, 3.
- (37) Briseno, A. L.; Tseng, R. J.; Li, S. H.; Chu, C. W.; Yang, Y.; Falcao, E. H. L.; Wudl, F.; Ling, M. M.; Chen, H. Z.; Bao, Z. N.; Meng, H.; Kloc, C. *Appl. Phys. Lett.* **2006**, *89*, 3.
- (38) De Vusser, S.; Steudel, S.; Myny, K.; Genoe, J.; Heremans, P. *Appl. Phys. Lett.* **2006**, *88*, 3.
- (39) Dzwilewski, A.; Wagberg, T.; Edman, L. *J. Am. Chem. Soc.* **2009**, *131*, 4006–4011.
- (40) Edman, L.; Ferry, A.; Jacobsson, P. *Macromolecules* **1999**, *32*, 4130–4133.
- (41) Wagberg, T.; Persson, P. A.; Sundqvist, B.; Jacobsson, P. *Appl. Phys. A* **1997**, *64*, 223–226.
- (42) Chambers, G.; Henderson, K.; Dalton, A. B.; McCarthy, B.; Byrne, H. J. *16th International Conference on Science and Technology of Synthetic Metals (ICSM 2000)*; Elsevier Science Sa: Gastein, Austria, 2000; pp 1111–1112.
- (43) Morales-Saavedra, O. G.; Castaneda, R.; Banuelos, J. G.; Carreon-Castro, M. D. *J. Nanosci. Nanotechnol.* **2008**, *8*, 3582–3594.
- (44) Hebard, A. F.; Eom, C. B.; Fleming, R. M.; Chabal, Y. J.; Muller, A. J.; Glarum, S. H.; Pietsch, G. J.; Haddon, R. C.; Mujsce, A. M.; Paczkowski, M. A.; Kochanski, G. P. *Appl. Phys. A* **1993**, *57*, 299–303.
- (45) McGinnis, S.; Norin, L.; Jansson, U.; Carlsson, J. O. *Appl. Phys. Lett.* **1997**, *70*, 586–588.
- (46) Dzwilewski, A.; Wagberg, T.; Edman, L. *Phys. Rev. B* **2007**, *75*, 075203.
- (47) Edman, L.; Swensen, J.; Moses, D.; Heeger, A. J. *Appl. Phys. Lett.* **2004**, *84*, 3744–3746.
- (48) Guo, T. F.; Wen, T. C.; Pakhomov, G. L.; Chin, X. G.; Liou, S. H.; Yeh, P. H.; Yang, C. H. *Thin Solid Films* **2008**, *516*, 3138–3142.
- (49) Brown, P. J.; Thomas, D. S.; Kohler, A.; Wilson, J. S.; Kim, J. S.; Ramsdale, C. M.; Sirringhaus, H.; Friend, R. H. *Phys. Rev. B* **2003**, *67*, 16.
- (50) Chirvase, D.; Parisi, J.; Hummelen, J. C.; Dyakonov, V. *Nanotechnology* **2004**, *15*, 1317–1323.

JP909216A